ANNALI DI GEOFISICA, VOL. 41, N. 4, October 1998

The Al Hoceima earthquake of May 26, 1994 and its aftershocks: a seismotectonic study

Sidi Otman El Alami([1]), **Ben Aissa Tadili**([1]), **Taj-Eddine Cherkaoui**([1]), **Fida Medina**([2]), **Mohamed Ramdani**([1]), **Lahcen Aït Brahim**([3]) **and Mimoun Harnafi**([1])

([1]) *Institut Scientifique, Département de Physique du Globe, Agdal, Rabat, Maroc*

([2]) *Institut Scientifique, Département de Géologie, Agdal, Rabat, Maroc*

([3]) *Faculté des Sciences, Département de Géologie, Rabat - R.P., Maroc*

Abstract

The present paper focuses on the moderate earthquake that occurred on May, 26, 1994, at 8 h 27 min, which caused great damage and two deaths. The epicentre of the main shock was located at 35.28°N, 3.99°W. The focal depth was 13 km, and the magnitude (M_d) attained 5.6. A field survey of the earthquake effects showed that the maximal intensity (VIII-IX EMS) follows an elongated corridor trending NNE-SSW, where 80% of the constructions were destroyed. During the 14-day survey carried out with the help of the temporary network established in the area, 512 shocks were located. The best constrained epicentres (68) are shallow and are largely distributed over a NNE-SSW trending cluster along an almost-vertical plane. Focal mechanisms determined for the main shock and for the 7 largest aftershocks, correspond to strike-slip faulting with a reverse (main shock and one aftershock) or normal component (6 events). The *P* axes have a NNW-SSE trend, with variable plunge, whereas the *T* axes are ENE-WSW with a slight plunge. The state of stress determined with the help of these mechanisms corresponds to a strike-slip regime with σ_1 oriented NNW-SSE and σ_3 ENE-WSW, which is in conformity with previous studies. The present study also shows that the Nekor fault remained inactive during the seismic crisis of 1994, as during the previous surveys, and this casts some doubt on the present-day role of this major fault. Instead, as proposed by some authors, a seismic zone trending NNE-SSW may be related to the faults of the same trend that appear to cross the Al Hoceima area towards the Alboran Sea.

Key words *seismicity – focal mechanisms – seismotectonics – geodynamics – Morocco – Rif*

1. Introduction

The present-day structure of the Western Mediterranean is the result of the convergence of the African and Eurasian plates along a NNW-SSE trend, at a rate close to 0.5 cm/yr around a pole situated near the Canary Islands (Minster and Jordan, 1978; Argus *et al.*, 1989; Demets *et al.*, 1994). This convergence is in part accommodated by a seismic activity that extends at its western segment from the Azores to the area situated between Southern Iberia and Northern Morocco, with a maximal frequency in the area of Al Hoceima (fig. 1). In this region, the study of the instrumental seismicity from 1901 to 1993 shows moderate seismicity, with magnitudes and felt intensities rarely exceeding 5 and VI (MSK) respectively (Cherkaoui, 1991). Earthquake foci are shallow, and mechanisms determined from tele-

Mailing address: Dr. Sidi Otman El Alami, Université Mohammed V, Institute Scientifique, Département de Physique du Globe, Av. Ibn Batouta, B.P. 703, Agdal, Rabat, Maroc; e-mail: elalami_otman@yahoo.com

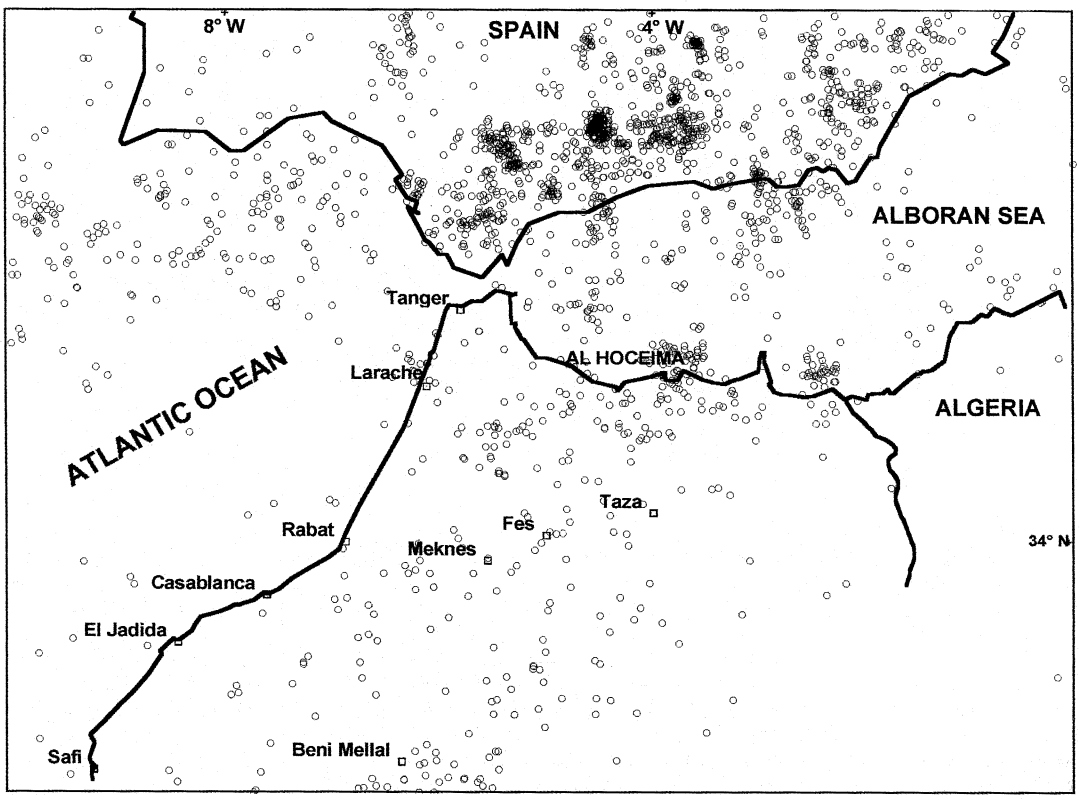

Fig. 1. Seismicity of Morocco and adjacent area from 1987 to 1993.

seisms and micro-earthquakes show horizontal, ENE-WSW trending tension axes, while the pressure axes are scattered within a NNW-SSE to NW-SE vertical plane (Hatzfeld, 1978; Frogneux, 1980; Medina and Cherkaoui, 1992; Hatzfeld *et al.*, 1993; Medina, 1995), thus indicating a heterogeneous state of stress, where σ_3, horizontal, is oriented ENE-WSW, and σ_1 is vertical, oblique or horizontal and oriented NNW-SSE (Medina, 1995).

In order to add some new elements to the available data, the present paper, whose main ideas were presented during the sixth international forum on seismic zonation and the first Ibero-Maghrebien region Conference (El Alami *et al.*, 1996), focuses on the seismological and seismotectonic aspects of the Al Hoceima earthquake of May, 26, 1994, which appears as the largest event ever recorded in Northern Morocco, and on the following aftershock sequence as recorded by the stations of the Institut Scientifique. Finally, the geodynamic implications for this part of the Rif chain are rapidly examined. It is noteworthy that the same event has recently been studied by investigators of Cornell University (Calvert *et al.*, 1997); however, our study is basically different from theirs since:

1) it is based on data collected for two weeks on the field, with the help of a temporary network of portable stations installed one day after the main shock;

2) it focuses on the seismotectonic aspects and particularly on the focal mechanisms for the largest aftershocks and the derived state of stress.

2. General tectonic setting

From the geodynamic point of view, the major problems that have been much discussed during the two last decades are those relative to the deep mechanisms that originated the Alboran Sea, to which the Al Hoceima area is structurally linked (fig. 2A), and the real limit between Africa and Iberia. A large outline of the previous ideas can be found in recent papers published by Meghraoui *et al.* (1996) and Calvert *et al.* (1997), so we recall here only the main points.

With respect to the vertical motions, three mechanisms have been proposed for the origin of the Alboran basin: 1) passive subsidence related to *in situ* cooling of a thermal dome (*e.g.*, Weijermaars, 1988); 2) delamination of a thickened lithosphere (Platt and Wissers, 1989; Morley, 1992; Seber, 1995), and 3) orogene collapse related to body forces (Dewey, 1988). These vertical motions, that can be quantified through subsidence analysis (Watts *et al.*, 1992), do not seem to be reflected by the present-day seismicity, perhaps with the exception of the deep earthquakes (600 km) recorded near Granada in Southern Spain, which are thought to reflect stress release within a fragment of subducted lithosphere (*e.g.*, Buforn *et al.*, 1991).

Similarly, different models were proposed to explain the tectonics of the area in the context of the horizontal motions, *i.e.* the convergence between Northwestern Africa and Iberia, to which the observed seismicity is strongly related. The most recent models involving different mechanisms at variable scales, are: 1) a simple N-S convergence producing a E-W extension in the Alboran area (Buforn and Udias, 1991; fig. 2B); 2) distributed deformation with rotating blocks bounded by large strike-slip faults (Vegas, 1991; fig. 2C); 3) westward expulsion of both the Iberian and Moroccan blocks (Fonseca and Long, 1991; fig. 2D); 4) westward expulsion of the Alboran block (Rebai *et al.*, 1992; fig. 2E); 5) E-W shear zone extending from the Atlantic to the Algerian Tell (GALTEL zone), with blocks bounded by strike-slip faults, and rotated around a vertical axis (Meghraoui *et al.*, 1996; fig. 2F). These largely differing models reflect the complexity of the area as well as the lack of sufficient seismotectonic data that can be used to construct a reliable model.

3. Geological setting

Geologically, the area of Al Hoceima belongs to the Central Rif chain, which runs parallel to the northern coast of Morocco (fig. 2A). Near the city, the most important structures consist of southward-verging thrust sheets (fig. 3) which are, from the upper to the lower (*i.e.* from north to south): 1) the Bokkoya, with nappes of Palaeozoic terranes and their Mesozoic-Cenozoic cover; 2) the Tiziren unit, comprising Middle Jurassic to Early Cretaceous carbonates and flysch series (3000 m); 3) the Ketama metamorphic unit, which consists of Cretaceous flysch and limestones. Volcanic rocks are represented by the middle Miocene Ras-Tarf andesites (Guillemin and Houzay, 1982).

In addition to the Nekor fault, which is considered a major transverse structure (*e.g.*, Leblanc and Olivier, 1984), the most important faults are:

1) The Imzouren (NNW-SSE) and Trougout (N-S) faults, which respectively delimit the western and eastern boundaries of the lower Nekor graben, filled by up to 400 m of Quaternary alluvial deposits. The Trougout fault is thought to extend offshore into the Al Hoceima Bay (Calvert *et al.*, 1997).

2) The Jbel Hammam fault system (NNW-SSE), consisting of several normal faults with trace lengths of 20 km.

3) The Rouadi fault, trending NNE-SSW over 15 km.

Other faults are visible within the Ketama unit east of Jbel Hammam and southeast of Targuist and within the Bokkoya unit. The most conspicuous of these is the NE-SW trending Bousekkour-Arhbal fault (fig. 3, BA), which crosscuts the whole Bokkoya unit, with a sinistral displacement (Mourier, 1982).

Most authors agree that, after the pre-Messinian emplacement of the Rif nappes, normal and strike-slip motion along the faults was

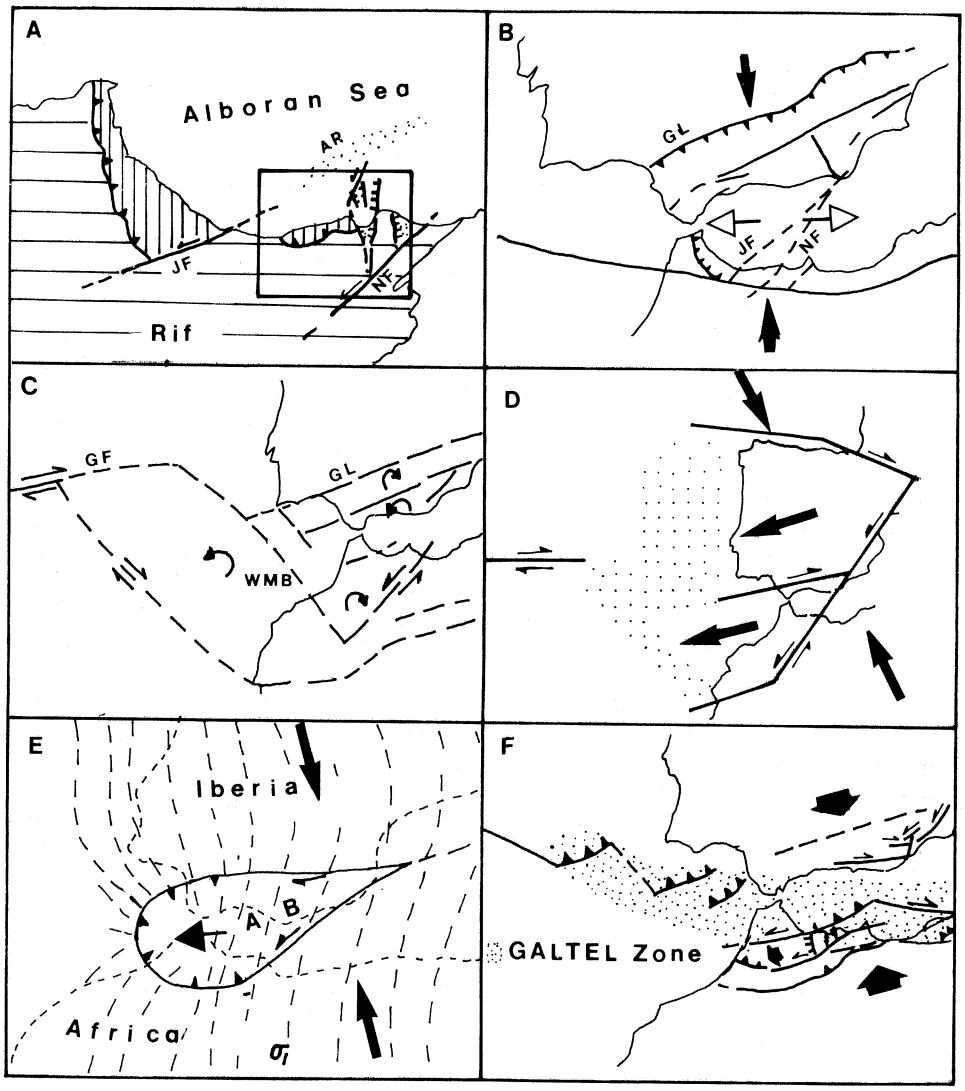

Fig. 2. Location of the Al Hoceima area, and some selected models depicting the present-day geodynamics (at different scales) of the Western Mediterranean. A = Location of the Al Hoceima area in Northern Rif. Area with vertical lines: internal zones; area with horizontal lines: external zones; dotted area (onshore): recent (Late Miocene to Plio-Quaternary) basins. B to F = Geodynamic models for the Western Mediterranean and Atlantic area involving different processes such as: B) simple convergence (Buforn and Udias, 1991); C) distributed deformation associated to rotation within blocks (Vegas, 1991); D) and E) expulsion tectonics (D from Fonseca and Long, 1991; E from Rebai *et al.*, 1992); F) complex E-W shear zone with rotations and expulsion (Meghraoui *et al.*, 1996). JF = Jebha Fault; NF = Nekor Fault; AR = Alboran Ridge; GL = Guadalquivir Lineament; GF = Gloria Fault; WMB = West Moroccan Basin; AB = Alboran Block; GALTEL = Gloria-Alboran-Tell zone. The thick arrows indicate the sense of motion of plates and small blocks. Thin arrows along faults correspond to lateral motion on fault plane. Other symbols are those conventionally used in structural maps.

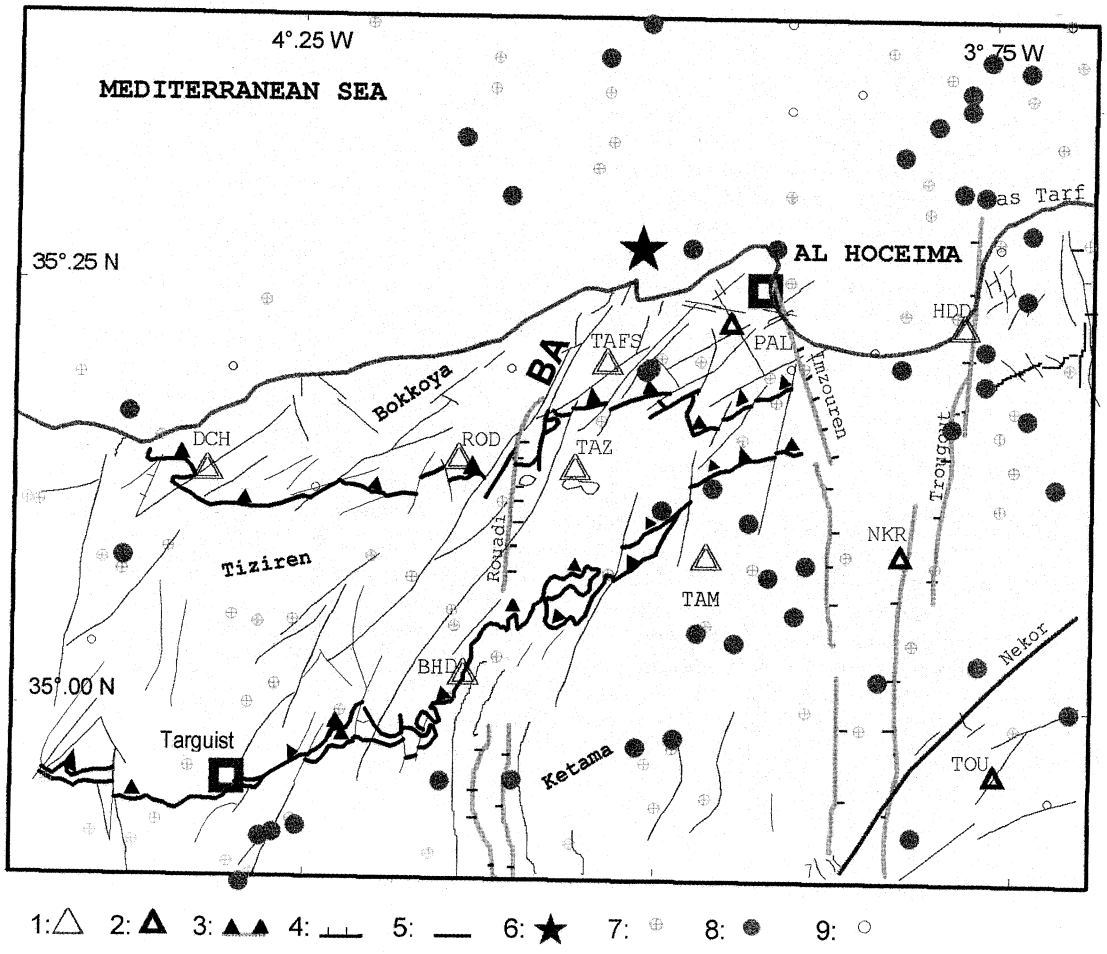

Fig. 3. Seismicity (1901 to 1993) and structural units of the Al Hoceima area. 1 = Temporary network station; 2 = permanent network station; 3 = thrust fault; 4 = normal fault; 5 = strike slip fault; 6 = the main shock; 7 = $M_d \leq 3.5$; 8 = $M_d > 3.5$; 9 = M_d not determined.

predominant. Structural analysis carried out by Frizon de Lamotte (1982, p. 297) and Chotin and Aït Brahim (1988) shows that a horizontal σ_1 underwent a counterclockwise rotation: ENE-WSW during the Tortonian, NNE-SSW during the end-Tortonian, and NW-SE in the Plio-Quaternary, even though a more complex evolution involving extensional episodes is inferred from local studies (Groupe de Recherche Néotectonique de l'Arc de Gibraltar, 1977).

4. Seismicity of the Al Hoceima area

The Al Hoceima region suffered in the past numerous earthquakes, many of which were felt by the population and caused severe damage (Galbis Rodriguez, 1932, 1940; Roux, 1934; Mezcua and Martinez Solares, 1983; Vogt, 1985; Ramdani *et al.*, 1989; Elmrabet, 1991; Levret, 1995). On the basis of the data collected from the catalog compiled by

Cherkaoui (1988) and the national seismological bulletins, 147 earthquakes were selected from 1901 to 1993, and their epicentres plotted in the area depicted in fig. 3. Seismicity appears diffuse due certainly to: 1) the high uncertainty on the epicentral determination, itself related to the large distance to the stations of the national seismic network until the late 1980s; 2) the fact that the Rif is strongly fractured, and moderate earthquakes can occur on different fault planes separately in time. Most of the seismic events are shallow, and their magnitudes do not exceed 5.5.

5. Characteristics of the main shock

The main shock of the 1994 seismic crisis occurred on May 26, 1994, at 8 h 27 min UTC, and strongly affected the city of Al Hoceima and the surrounding regions, causing two deaths and important material damage. The epicentre of the earthquake was relocated by this study offshore north of Al Hoceima (35.28°N, 3.99°W), with a magnitude M_d of 5.6 (M_w = 6.0), and a depth of 13 km (fig. 4, epicentre 1). However, it should be emphasized that the position of the epicentre and the depth of the event are not well constrained, because of the configuration of the seismological network and the complex deep structure of the Rif (table I).

Table I. Velocity model used.

Depth (km)	0.0	15	30	100	200	300
V_p (km/s)	6.1	6.7	8.0	8.2	8.3	8.58

Different epicentre determinations were proposed for the main shock (fig. 4 and table II). The nearest ones to the aftershock sequence location are epicentres 1 (this study), 10 (Calvert *et al.*, 1997) and 6 (CNRM). For a detailed discussion on the problem of the epicentre determination, the reader is referred to Calvert *et al.* (1997, pp. 641-643).

The seismic moment M_o was estimated by NEIC at $9{,}17.10^{17}$ N · m and by Harvard at 1.10^{18} N · m and the main shock had been preceded since 1 May 1994 by many foreshocks, seven of which had magnitudes (M_d) of 2.9 to 3.8.

Table II. The epicentral determinations for the main shock, proposed by different authors and international centres.

No.	Source	Lat. °N	Lon. °W	M_b	M_d	M_w	Depth (km)
1	This study	3.99	35.28		5.6		13
2	LIS	3.97	34.99	5.3			73
3	NEIC	4.1	35.31	5.7			10
4	MOS	4.05	35.46	5.9			10
5	MDD	4.03	35.3	5.7			3
6	CNRM	3.91	35.14		5		21
7	DPG	4.17	35.31		5.6		30
8	HRVD	3.91	35.37			6.0	15
9	ISC	4.12	35.28		5.5		11
10	Calvert *et al.* (1997)	3.955	35.159				
11	BJI	3.93	35.72		5.6		7

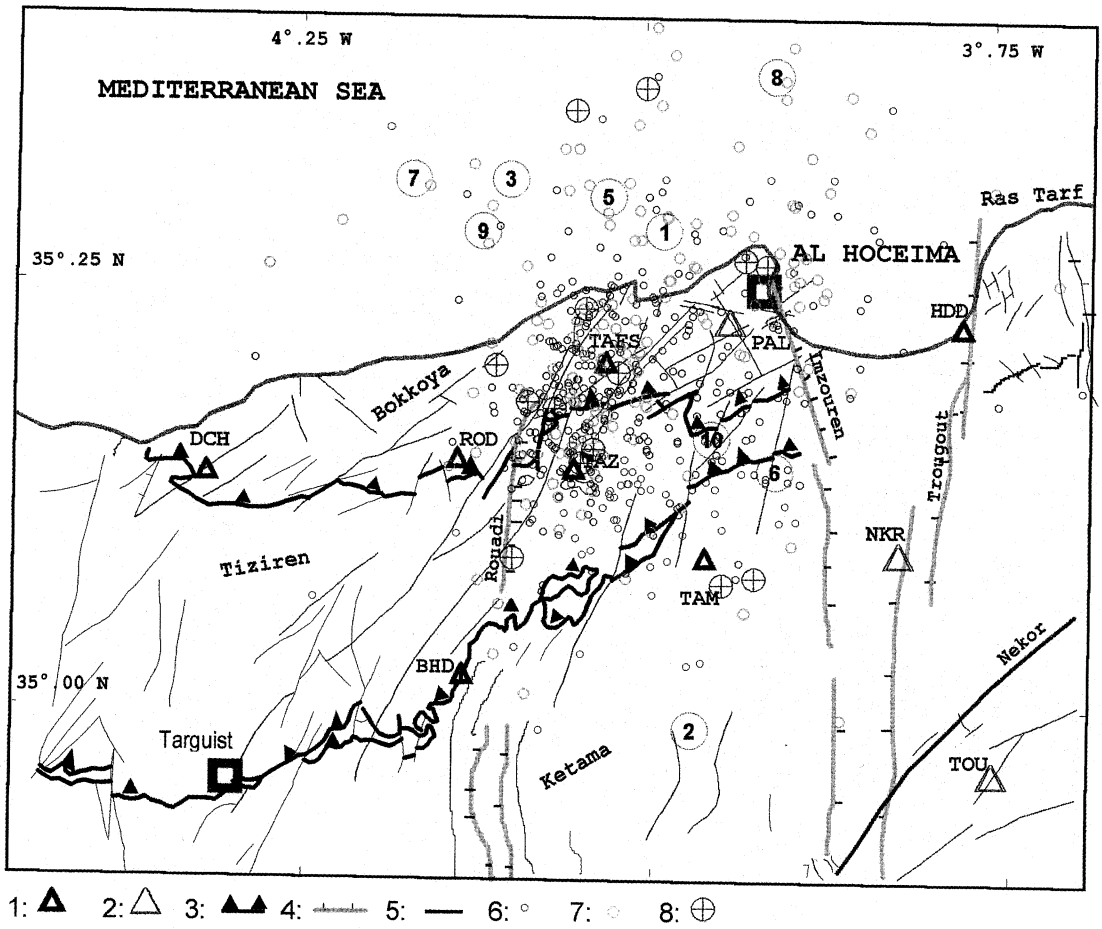

Fig. 4. Locations of the epicentre of the Al Hoceima main shock (numbered circles) and distribution of the 512 aftershocks from 27 May to 9 June 1994. Symbols 1 to 5 as in figs. 3: 6 = $M_d \leq 2.5$; 7 = $2.5 < M_d \leq 3.5$; 8 = $3.5 < M_d \leq 4.5$.

6. Macroseismic study

Data collected during the macroseismic study carried out on the field just after the main shock, allowed us to draw an isoseismal map (fig. 5) based on EMS 1992 scale (Working Group on Macroseismic Scale, 1993).

This map shows that maximal damage occurred within a NNE-SSW narrow elongated area between 35.25°N, 4°W and 35.12°N, 4.15°W, enclosing the localities of Rouadi, Tazarine, Arhbâl, Tafensa, Idssouliyen and Boussekkour, for which intensity VIII-IX (EMS) was assigned. All constructions located in this zone were destroyed at least by 80% (photograph 1). The other isoseismal lines in fig. 5 are elongated in the same direction, and strongly suggest that the fault which generated the main shock, may have the same trend. The nearest fault to the maximal intensity zone is the Boussekkour-Arhbal fault (fig. 3, BA), which has the same trend as the isoseismal lines. However, as the depth of focus is about 13 km, it is difficult to state, in the absence of

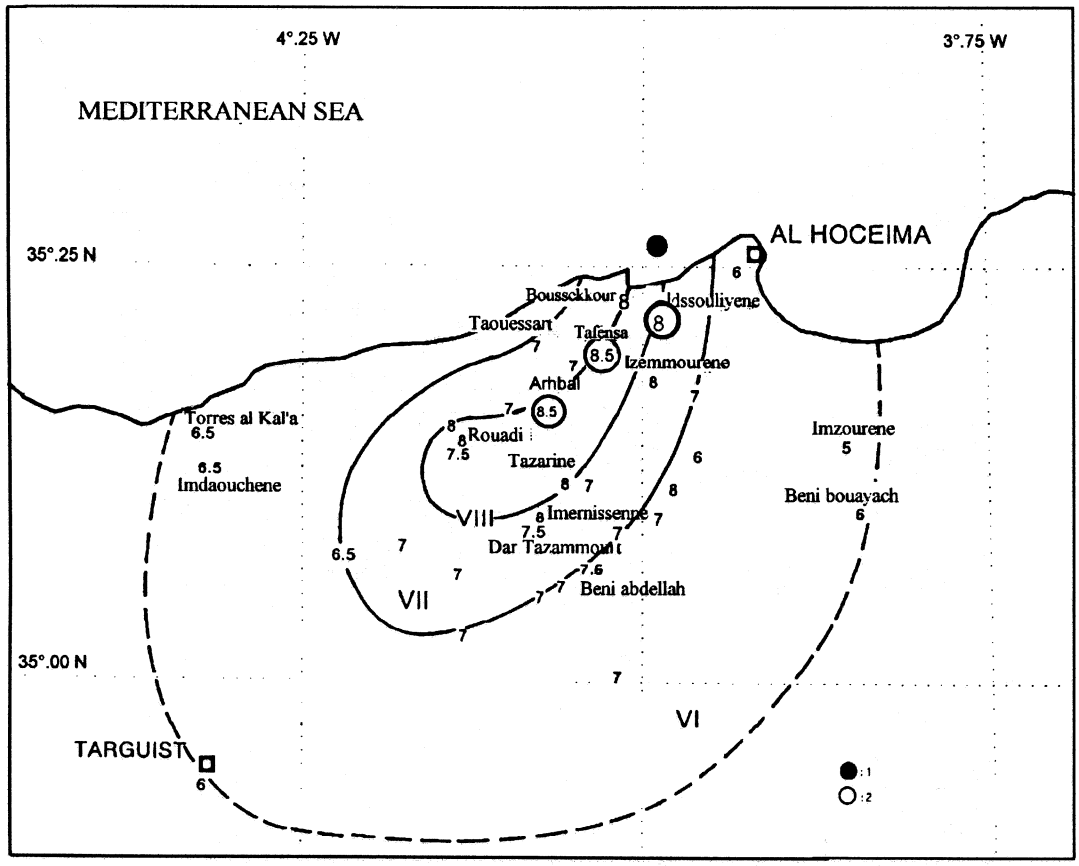

Fig. 5. Isoseimal map of the Al Hoceima main shock of May, 26, 1994 (field observations by S.O. El Alami and B. Tadili) and location of photographs 1 at Tafensa, and 2 at Idssouliyene. 1 = Location of the main shock; 2 = location of observed fissuration.

seismic profiles, that this fault plane was reactivated, because this would indicate that the fault plane extends to 13 km in depth and is not offset by subhorizontal decoupling surfaces (decollements and thrust planes). An alternative view is to consider that the maximal damage was due to a site effect within the valley that extends along the fault trace.

As a consequence of the main shock, some effects were observed at the surface, such as decametric-scale *en échelon* fissures at Idssouliyene, Tafensa and Arhbâl (fig. 5 and photograph 2), with a N40 to N50 trend, and landslides along the coastal cliffs west of Al Hoceima, at Ras El Abid and Kimmat Inassinene. Other landslide structures were observed at Tafensa, Tenda Ifrane and at Jbel Boubrhel. However, no faults of unequivocal character were observed during the survey.

7. Aftershock survey

The temporary network, consisting of seven analogic stations (vertical component, with a period of 1 s), was installed one day after the

Photograph 1. Example of a construction that was almost-completely destroyed by the earthquake of May, 26, 1994 (Douar of Tafensa). Location in figs. 4 and 5.

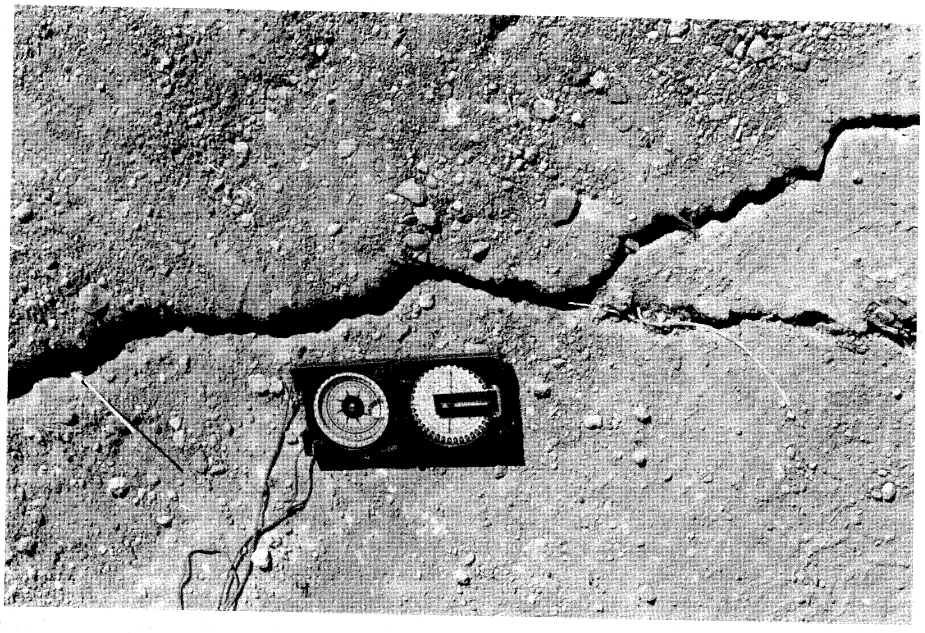

Photograph 2. Example of a surface fracture trending N40°, that appeared during the earthquake of May, 26, 1994 in the Idssouliyene area, location in fig. 5.

main shock (27 May 1994). The configuration of the stations was chosen so as to cover the presumed epicentral area (fig. 4). For aftershocks with magnitudes M_d higher than 3, data were completed with those taken from the permanent networks of Morocco, Spain and Portugal. For small aftershocks (magnitude $M_d < 1.5$), only those recorded by at least 3 stations were taken into account. A detailed study of the aftershock sequence of the Al Hoceima earthquake was also performed by Calvert *et al.* (1997); however, their work was mainly based on data collected from teleseisms recorded by the permanent digital stations of the Centre National de la Recherche (CNRM), and cover the period from October 1993 to June 1994, whereas the present study was performed with the help of temporary analogic stations and concerns a shorter period (two weeks).

From May 27 to June 9, 1994, our network recorded a very large number of small events (fig. 4), 512 of which were determined with the help of the HYPO71 program (Lee and Lahr, 1975). In order to include data from the permanent networks, we used the standard velocity model for Morocco (table I), with $V_p/V_s = 1.74$. The variation in the position of the epicentre is small with respect to the variation of the ratio V_p/V_s (Christodoulou, 1986). The mean RMS of 512 aftershocks, was estimated at 0.34 ± 0.2 s.

Magnitudes of aftershocks were evaluated by the formula

$$M_d = -1.258 + 2.132 \log(\tau) + 0.007\,\Delta \quad (7.1)$$

where the constants were calculated by the least squares method, using 26 data recorded by Tafensa (TAFS) and the seismic permanent network of Morocco. For the latter, the constants are those determined by Frogneux (1980) for $M_d \leq 4$, and by Cherkaoui (1991) for $M_d > 4$, who calibrated Magnitudes M_d against magnitudes m_b determined by the ISC and USGS. The mean quadratic error on magnitudes is ± 0.2.

The histogram in fig. 6 represents the number of aftershocks per day, with the corresponding maximal magnitude. The largest number of aftershocks was recorded from May, 30 to June, 3, with the highest magnitude M_d being 4.4.

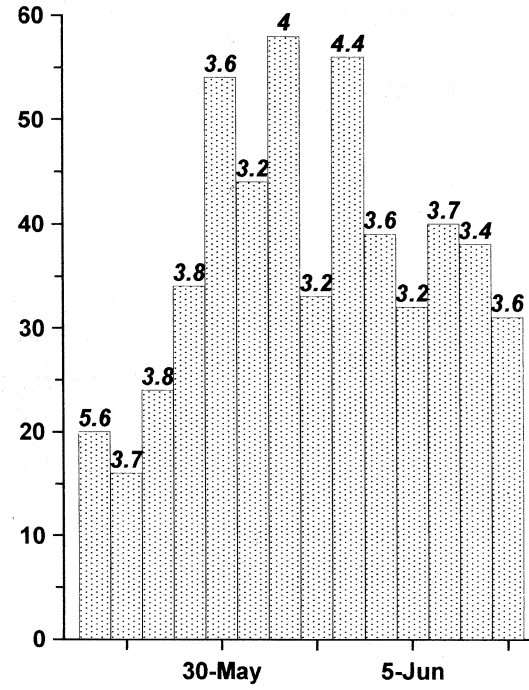

Fig. 6. Temporal distribution of the aftershocks from 27 May to 9 June 1994. The numbers above the bars correspond to the recorded maximal magnitudes per day.

All the recorded aftershocks are plotted in fig. 4 without taking into account any kind of constraints. This map shows that most of the epicentres are located onshore; however, it is not possible to find any correlation between the aftershocks and the tectonic features. If we only select the events with RMS less or equal to 0.25, and with error on depth and epicentre less than 2 km, this leaves 68 aftershocks (fig. 7), with most events around Tafensa. The epicentres are widely distributed over a NNE-SSW trending cluster, about 30 km long and 10 km wide, that fits with the direction where maximal damage was observed (fig. 5). The aftershocks appear southwards of the epicentre of the main shock when the latter is taken to be offshore. This shift may be due either to errors on the determination of the main shock epicen-

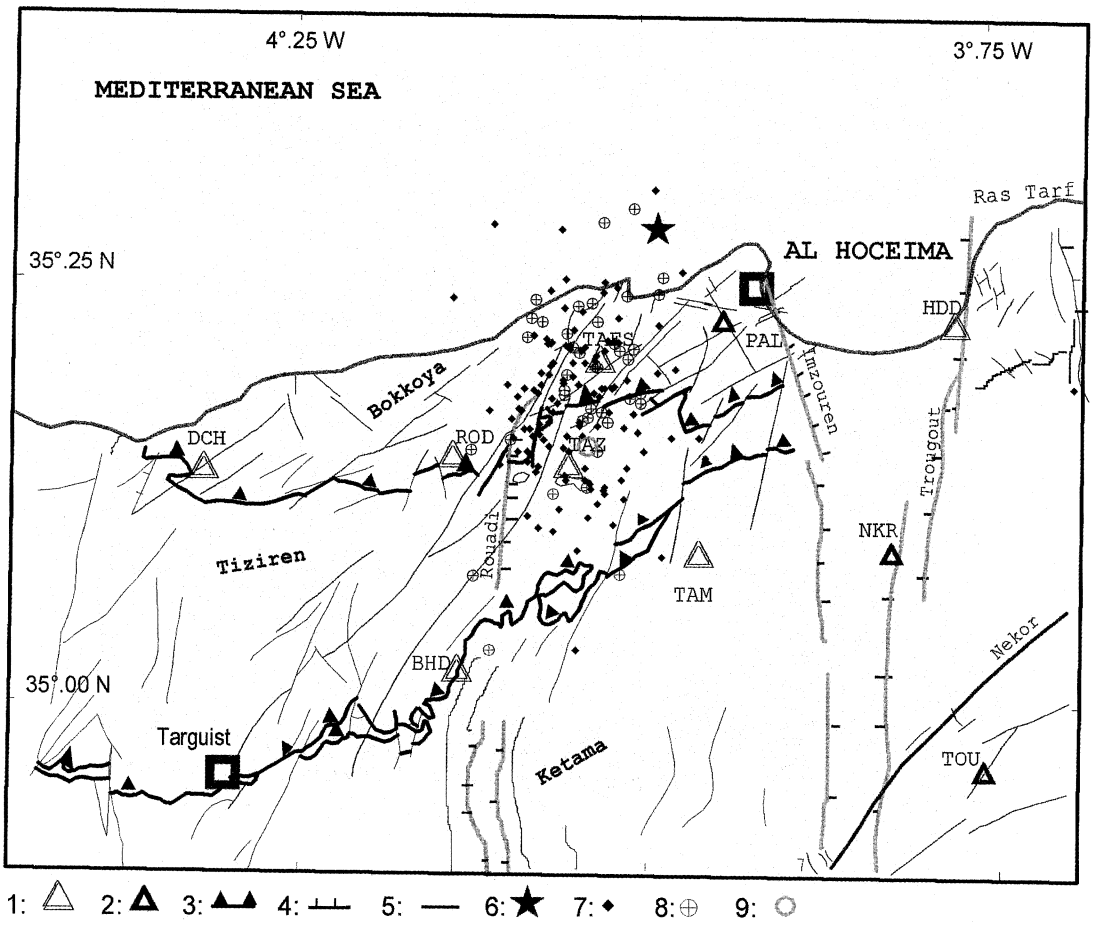

Fig. 7. Distribution of selected aftershocks (n = 68) with RMS less than 0.25 s and with errors on depth less than 2 km. Symbols 1 to 5 as in fig. 3; 6 = location of the main shock; 7 to 9 = epicentres of the aftershocks (size is proportional to magnitude as in fig. 4).

tre, or to sensitivity threshold of the seismic stations, which would not record weak events located in the offshore Bokkoya basin.

It is important to note here that the aftershock cluster appears to the west of that shown by Calvert *et al.* (1997). We think that this may be due to the use of different data sources which introduce some shift in the location of the epicentres, and has no geologic significance (an eastward shift in fault activity, for instance).

In order to investigate the possible existence of a seismogenic fault, the epicentres of aftershocks were projected onto vertical sections oriented at different angles to the NNE-SSW trending cluster. Among all the sections, the one oriented WNW-ESE, perpendicular to the cluster, suggests that the foci are concentrated along a plane with a steep dip to the east-northeast (fig. 8). The other sections do not show any preferred orientation of foci. Most events are 2 to 18 km deep. It is important to

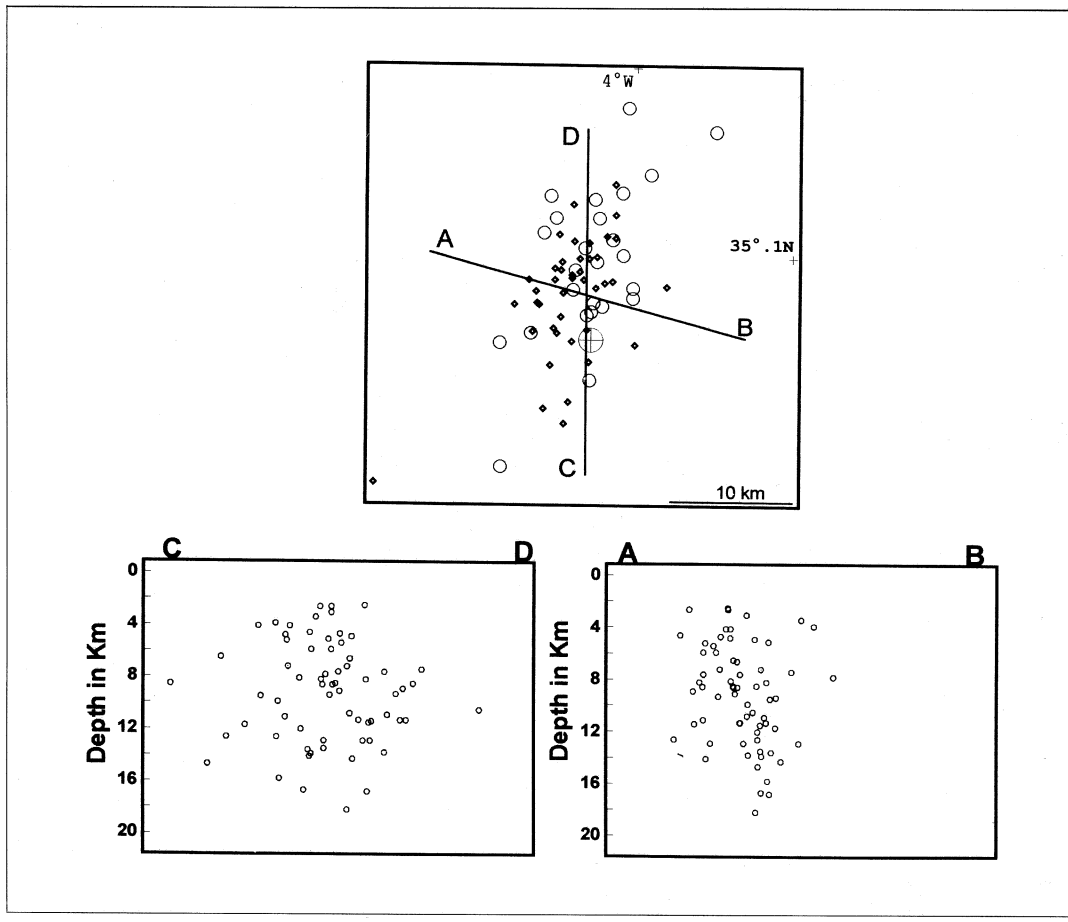

Fig. 8. Cross-sections of the aftershock cluster of the Al Hoceima earthquake.

note that the trend of this fault is very different from that of the Bousekkour-Arhbal fault, which is suggested by the isoseismal map.

8. Focal mechanisms

P-wave first motions for the main shock were read from seismograms of the permanent seismic network of Morocco and the Ibero-Maghrebian countries. For distant stations, we used readings from the ISC bulletin, for selected stations with *iP* arrivals. Aftershocks were studied with data provided both by temporary and permanent seismic networks. Quality of readings was variable: while the first motions on analog records of the Moroccan stations were relatively easy to determine, more difficulties were found with the Spanish digital seismograms, which sometimes yielded contradictory first motions. This problem, which was also found during previous studies (Medina and Cherkaoui, 1992) introduces some degree of uncertainty in the focal mechanism solutions.

8.1. *Main shock*

Several solutions were determined for the main shock by different seismological centres (USGS, CSEM and Harvard), on the base of *P*-wave arrivals and waveform modelling (fig. 9 and table III). All show strike-slip motion with normal or reverse components, and a well constrained NNE-SSW trending plane. We also attempted to find a solution based on the *P*-wave arrivals, either by hand or using the computer program FPPLOT (Reasenberg and Oppenheimer, 1985). The best solution corresponds to strike-slip motion with a reverse component. The first plane, sinistral, is oriented 202, 60°, whereas the second, dextral, is 100, 72°. The *P* axis plunges slightly (6°) towards azimuth 152, the *T* axis is oriented 58, 37°.

The solutions given by Harvard (*P* waves), USGS (NEIC, 1995) and CSEM (Bock *et al.*, 1994) are slightly inconsistent with our data, since their southwestern quadrant is extensional (compressional first motions), while most readings of Moroccan stations show undoubtful dilatational first motions.

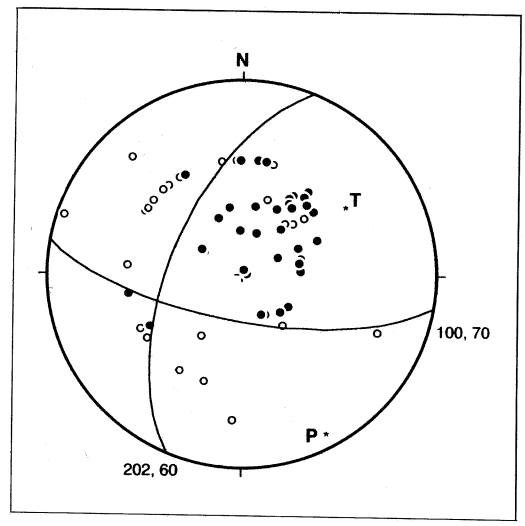

Fig. 9. Proposed solution for the focal mechanism of the main shock of May, 26, 1994, based on *P*-wave arrivals. Empty circles = dilatations; solid circles = compressions; *P* = pressure axis; *T* = tension axis. The parameters of the axes are indicated in table II.

8.2. *Aftershocks*

Despite the great number of aftershocks, most events were too weak to be recorded by a sufficient number of stations. For this reason, the most reliable solutions are only seven (fig. 10 and table IV). The best solutions, obtained with the help of the computer program, correspond to strike-slip/normal faulting, except for the aftershock of June, 3, at 8 h 57 min, which shows a reverse component as for the main shock. All *T*-axes plunge slightly and are oriented NE-SW to ENE-WSW; the *P*-axes plunge moderately (60° maximum).

Table III. Parameters of planes (strike and dip) and axes (azimut and plunge) for the main shock of May, 26, 1994, according to different sources and to the present study.

Plane A str. (°)	dip (°)	Plane B str. (°)	dip (°)	*P*-axis az. (°)	pl. (°)	*T*-axis az. (°)	pl. (°)	Reference
93	75	00	80	316	18	47	04	USGS (*P*-Waves)
93	80	02	84	317	11	47	03	USGS (*M*-Tensor)
112	48	17	85	326	33	72	24	HARVARD (CMT)
91	83	00	87	316	14	224	04	HARVARD (*P*-Waves)
291	86	200	79	156	11	67	05	EMSC
202	60	100	72	152	06	58	37	This paper

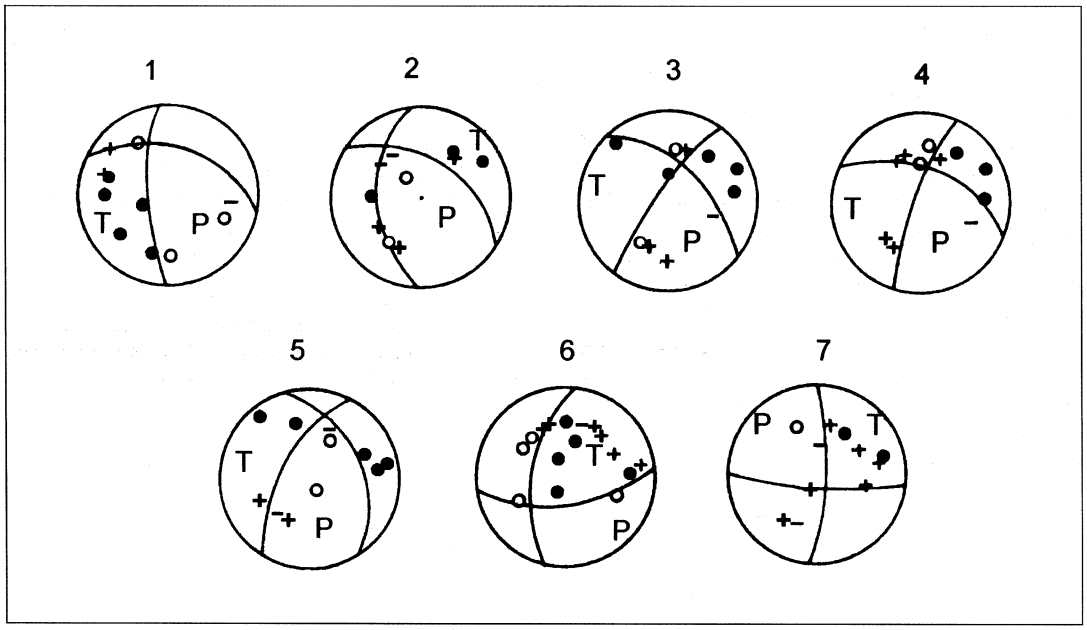

Fig. 10. Focal mechanisms of the main aftershocks of the Al Hoceima earthquake. Symbols as in fig. 9. Plus and minus signs correspond to poor quality readings (compressional and dilational first motions respectively). The characteristics of the events and the parameters of planes and axes are given in table IV.

Table IV. List of the aftershocks used in this study and focal mechanism solutions. NS = number of stations used (between brackets, number of inconsistent data).

							Plane A		Plane B		*P*		*T*		
No.	Date	Time	Lat.	Lon.	h	Mag.	ϕ	δ	ϕ	δ	Az	Pl	Az	Pl	NS(I)
1	26-5-94	12-27-54	35°12′	4°01′	20	4.4	185°	70°	298°	44°	140°	49°	247°	15°	13(1)
2	28-5-94	03-32-02	35°14′	4°03′	10	3.5	180°	50°	308°	54°	159°	60°	063°	03°	10(1)
3	29-5-94	19-14-05	35°14′	4°02′	10	3.3	220°	80°	316°	60°	174°	29°	270°	19°	11(3)
4	29-5-94	23-45-06	35°16′	4°02′	10	4.0	199°	82°	296°	56°	146°	37°	254°	23°	11(1)
5	01-6-94	00-53-52	35°11′	4°01′	8.5	4.0	209°	64°	330°	43°	166°	55°	273°	13°	11(1)
6	03-6-94	08-57-38	35°11′	4°02′	8	4.6	190°	55°	082°	66°	138°	07°	040°	44°	21(5)
7	08-5-94	03-08-31	35°11′	4°02′	10	3.6	008°	80°	100°	80°	324°	14°	234°	01°	11(1)

8.3. *State of stress*

Relying on these data, we tried to determine the state of stress numerically with the stress tensor inversion method, in particular the R4DT four-dimensional exploration (Angelier, 1984) with the help of the unpublished computer program developed by Jacques Angelier. Solutions were weighted from 1 to 8 according to the magnitudes of the corresponding events.

In a first computation, we considered both nodal planes in each solution as faults. This allowed us to obtain the directions of the principal stress axes (σ_1 at N142, 20°, σ_2 at N342, 69° and σ_3 at N234, 07°) with a ratio $\Phi = (\sigma_2 - \sigma_3/\sigma_1 - \sigma_3)$ of 0.225.

From this first determination, we tried to distinguish, within each solution, the main fault plane from the auxiliary one by selecting the nodal planes whose slip vector showed the smallest angular deviation from the calculated shear stress (Angelier, 1984). Unexpectedly, most planes oriented E-W to NW-SE appear to be the main fault planes. However, the slip vectors on the nodal planes in the mechanisms of the main shock and No. 4 show very small angular differences, so that the choice of the main fault plane cannot be considered unequivocal. After this selection, the same computation was repeated. This gave the orientation of the stress axes, with σ_1 at N140, 19°, σ_2 at N270, 62° and σ_3 at N42, 20° (fig. 11). However, it can be readily noticed that introducing this selection does not dramatically change the parameters of the principal stress axes.

In sum, the studied mechanisms show the predominance of strike-slip faulting with a normal or reverse component, and are perfectly compatible with the present-day NNW-SSE compression and ENE-WSW extension, determined in the area as a response to the convergence between Africa and Iberia (Medina, 1995).

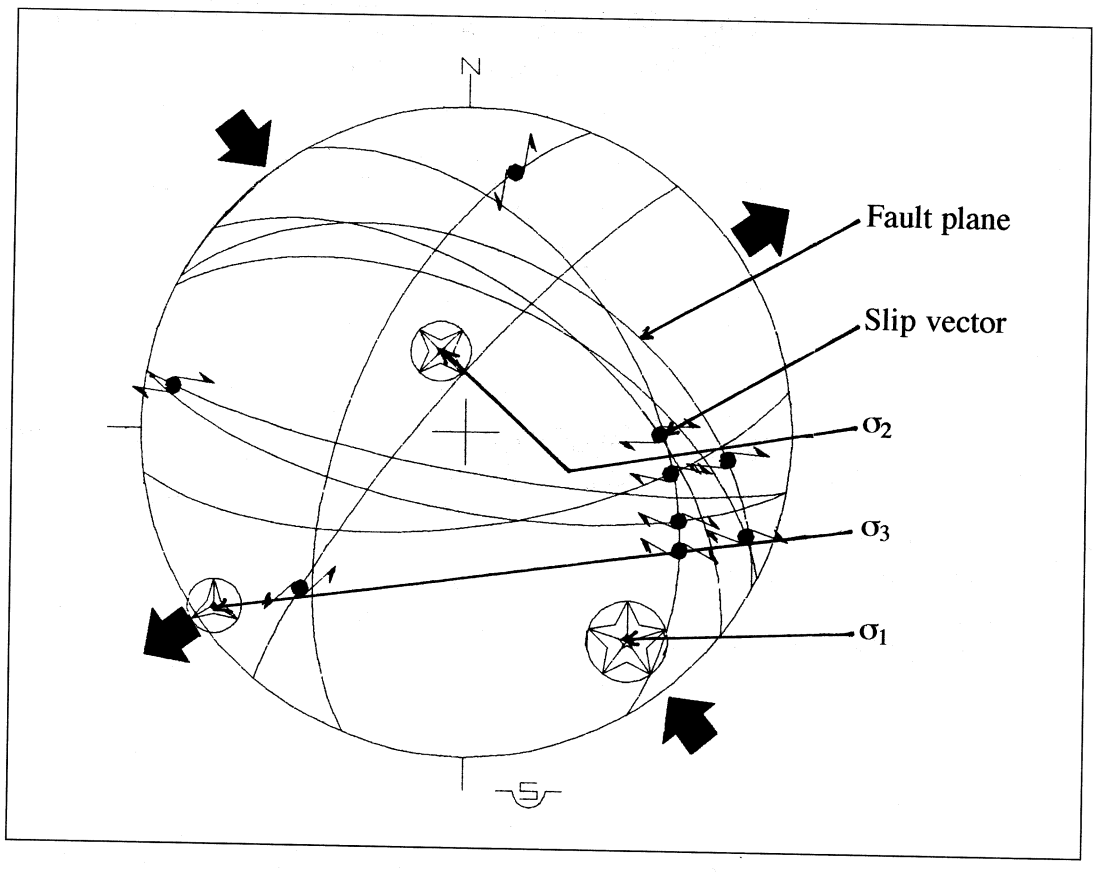

Fig. 11. Determination of the orientation of the main stress axes with the help of a quadridimensional grid search (Angelier, 1984).

9. Discussion

The study of the Al Hoceima earthquake and its aftershock sequence emphasizes many geological characteristics of the area. Thus, the recorded seismicity does not appear to be related to the Nekor fault, which remains inactive at the present time, as also shown by the studies carried out earlier (Frogneux, 1980; Cherkaoui *et al.*, 1990; Hatzfeld *et al.*, 1993; Calvert *et al.*, 1997). The distribution of the aftershocks corresponds to an elongated strip oriented NNE-SSW but not to isolated sources as in the former microseismic study of Cherkaoui *et al.* (1990).

On the base of aftershock distribution, focal mechanism solutions and effects in the field, we interpret this pattern as due to a zone of major faulting of strike-slip and normal displacements (fig. 12). This interpretation is not new, since it has already been proposed that, in the Alboran area, seismicity follows a NNE-SSW trend extending from Almeria in Southern Spain to Al Hoceima. In particular, Dillon *et al.* (1980) suggested a fractured zone with vertical faults affecting the recent sediments of the Alboran Sea, to which they correlate the observed seismicity. This interpretation has been in part recently confirmed by Calvert *et al.* (1997), who, however, suggest that this

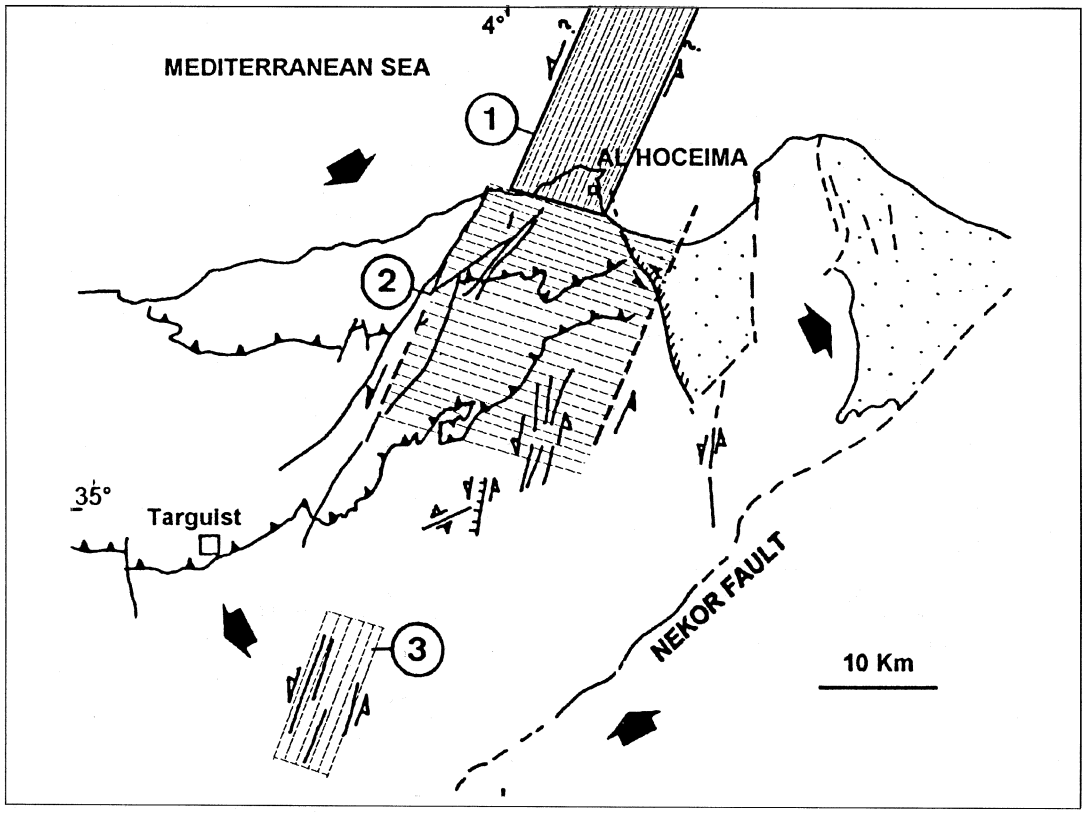

Fig. 12. Proposed sketch for the present-day activity of the faults in the Al Hoceima area, showing NNE-SSW oriented left-lateral strike-slip corridors. 1 = After Dillon *et al.* (1980); 2 = after this study; 3 = after Cherkaoui *et al.* (1990).

zone is interrupted at its northern border by the Alboran ridge and does not extend to Southern Spain. We consider that our results support the existence of this cross-element, taking into account that the fracture zone suggested by seismicity is obviously deeper (2 to 18 km) than that inferred from seismic-reflection studies. However, it is difficult to state whether the zone extends or not to the Spanish coast because of the detection threshold of the network.

The fact that the focal mechanism of the main shock has a reverse component and the aftershock mechanisms are rather strike-slip with a normal component is not surprising, since the area is characterized by distributed deformation (Hatzfeld *et al.*, 1993; Calvert *et al.*, 1997) with a heterogeneous state of stress, where the stress axes may often undergo rotations and permutations. In addition, it is known that large strike-slip zones may include normal or reverse faults, especially within releasing and restraining bends and rotating blocks. However, it can be readily noticed that the mechanisms of the largest events in the area are strike-slip with a reverse component, whereas the smallest have a rather normal component. This may suggest that during the main shocks, strike-slip faults are reactivated within a regional (mean) state of stress, whereas the aftershocks with a normal component correspond to re-adjustments of displaced blocks within a local state of stress, as proposed by Carey-Gailhardis and Mercier (1992).

The earthquake of May, 26, 1994, confirms the results of the seismic hazard study in the Al Hoceima region, for which Cherkaoui (1991) estimates the centennial intensities susceptible to be exceeded, at about VI to VII (MSK). For the same region, Tadili (1991) evaluates the soil accelerations at 26% *g*, corresponding to a probability of 90%, not to be exceeded, for a period of 100 years.

10. Conclusions

The present paper has focused on the moderate earthquake that occurred on May, 26, 1994, at 8 h 27 min.

1) The epicentre was located at 35.28°N, 3.99°W. The focal depth was 13 km, and the magnitude (M_d) attained 5.6.

2) The maximal intensity (VIII-IX EMS) was observed within an elongated corridor trending NNE-SSW, where 80% of the constructions were destroyed. This corridor follows the trend of the Bousekkour-Arhbal fault.

3) During the 14-day survey carried out after the earthquake, 512 shocks were located by the temporary network established in the area. Applying constraints on epicentre location leaves about 68 shallow events, which are widely distributed over a NNE-SSW trending cluster.

4) Focal mechanisms determined for the main shock and 7 major aftershocks, correspond to strike-slip faulting with a reverse (main shock and one aftershock) or normal component (6 events). The *P* axes have a NNW-SSE trend, with variable plunge, whereas the *T* axes are ENE-WSW with a slight plunge. The state of stress determined with the help of these mechanisms corresponds to a strike-slip regime with σ_1 oriented NNW-SSE and σ_3 ENE-WSW, which is in conformity with previous studies.

5) The present study also shows that the Nekor fault remained inactive during the seismic crisis of 1994, as during the previous surveys, and this casts some doubt on the present-day role of this major fault. Instead, as proposed by some authors, a seismic zone trending NNE-SSW may be related to the faults of the same trend that appear to cross the Al Hoceima area, towards the Alboran Sea.

Acknowledgements

We would like to thank the Royal Gendarmery, the local authorities and the Marine Fisheries Delegation at Al Hoceima for their help, as well as Mr. Kassimi (CNCPRST) and Mr. Ikharrazen (Institute). We also thank our colleagues in Tunisia, the Ivory Coast and France for providing useful information and Prof. D. Giardini and an anonymous reviewer for their helpful comments.

REFERENCES

ANGELIER, J. (1984): Tectonic analysis of fault slip data sets, *J. Geophys. Res.*, **89** (B7), 5835-5848.

ARGUS, D.F., R.G. GORDON, CH. DEMETS and S. STEIN (1989): Closure of the Africa-Eurasia-North America plate motion circuit and tectonics of the Gloria Fault, *J. Geophys. Res.*, **94**, 5585-5602.

BOCK, G., W. HANKA and R. KIND (1994): EMSC rapid source parameter détermination, European-Mediterranean Seismological Centre, *Newsletter*, **6**, 1-4.

BUFORN, E. and A. UDIAS (1991): Focal mechanism of earthquakes in the Gulf of Cadiz, South Spain and Alboran Sea, *Publ. Inst. Geogr. Nac.*, Madrid, Série Monografia, No. 8, 28-40.

BUFORN, E., A. UDIAS, J. MEZCUA and R. MADARIAGA (1991): A deep earthquake under South Spain, 8 March 1990, *Bull. Seism. Soc. Am.*, **81** (4), 1403-1407.

CALVERT, A., F. GOMEZ, D. SEBER, M. BARAZANGI, N. JABOUR, A. IBENBRAHIM and A. DEMNATI (1997): An integrated geophysical investigation of recent seismicity in the Al-Hoceima region of North Morocco, *Bull. Seism. Soc. Am.*, **87** (3), 637-651.

CAREY-GAILHARDIS, E. and J.L. MERCIER (1992): Regional state of stress, fault kinematics and adjustments of blocks in a fractured body of rock: application to the microseismicity of the Rhine graben, *J. Struct. Geol.*, **14** (8/9), 1007-1017.

CHERKAOUI, T.E. (1988): Fichier des séismes du Maroc et des régions limitrophes 1901-1984, *Trav. Inst. Sci., Ser. Geol. Geogr. Phys.*, **17**, pp. 158.

CHERKAOUI, T.E. (1991): Contribution à l'étude de l'aléa sismique du Maroc, *Ph.D. Thesis*, Université Joseph Fourier, Grenoble, pp. 247.

CHERKAOUI, T.-E., D. HATZFELD, H. JEBLI, F. MEDINA and V. CAILLOT (1990): Etude microsismique de la région d'Al Hoceima, *Bull. Inst. Sci.*, Rabat, **14**, 25-34.

CHRISTODOULOU, A.A. (1986): Etude sismotectonique et inversion tridimensionnelle en Grèce du Nord, *Ph.D. Thesis*, Université Joseph Fourier, Grenoble, pp. 181.

CHOTIN, P. and L. AÏT BRAHIM (1988): Transpression et magmatisme au Néogène-Quaternaire dans le Maroc Oriental, *C. R. Acad. Sci.*, Paris, **306**, ser. II, 147-148.

DEMETS, C., R.G. GORDON, D.F. ARGUS and S. STEIN (1994): Effect of the recent revisions to the geomagnetic reversal time scale on the estimate of current plate motions, *Geophys. Res. Lett.*, **21**, 2191-2194.

DEWEY, J. (1988): Extensional collapse of orogens, *Tectonics*, **7**, 1123-1139.

DILLON, W.P., J.M. ROBB, H.G. GREENE and J.C. LUCENA (1980): Evolution of the continental margin of Southern Spain and the Alboran Sea, *Mar. Geol.*, **36**, 205-226.

EL ALAMI, S.O., B. TADILI, T.-E. CHERKAOUI, F. MEDINA, M. RAMDANI, L. AÏT BRAHIM and M. HARNAFI (1996): The main Al Hoceima earthquake of May, 26, 1994 and its aftershocks, in *Sixth International Forum on Seismic Zonation and First Ibero-Maghrebian Region Conference, Barcelona, December 16-18, 1996.*

ELMRABET, T. (1991): History of earthquakes in Morocco, *Troisième Cycle Thesis*, Univ. Mohammed V, Faculté des Lettres et des Sciences Humaines Rabat, pp. 370 (in Arabic)

FONSECA, G.B.F.D. and R.E. LONG (1991): Seismotectonics of SW Iberia: a distributed plate margin?, *Publ. Inst. Geogr. Nac.*, Madrid, Série Monografia, No. 8, 227-240.

FRIZON DE LAMOTTE, D. (1982): Contribution à l'étude de l'évolution structurale du Rif oriental, *Notes and Mem. Serv. Geol. Maroc*, **314**, 239-309.

FROGNEUX, M. (1980): La sismicité Marocaine de 1972 à 1978. Etude des paramètres à la source des séismes proches, *Troisième Cycle Thesis*, Univ. Grenoble, pp. 131

GALBIS RODRIGUEZ, J. (1932): Catalogo sismico de la zona comprendida entre los meridianos 5°E y 20°W de Greenwich y los paralelos 45° y 25°N. **I**; *Inst. Geogr. y Catastral*, Madrid, pp. 807.

GALBIS RODRIGUEZ, J. (1940): Catalogo sismico de la zona comprendida entre los meridianos 5°E y 20°W de Greenwich y los paralelos 45° y 25°N. **II**; *Inst. Geogr. y Catastral*, Madrid, pp. 207.

GUILLEMIN, M. and J.P. HOUZAY (1982): Le Néogène post-nappe et le Quaternaire du Rif Nord-Oriental. Stratigraphie et tectonique des bassins de Melilla, du Kert, de Boudinar et du piedmont des Kebdana, *Notes and Mem. Serv. Geol. Maroc*, **314**, 7-237.

GROUPE DE RECHERCHE NEOTECTONIQUE DE L'ARC DE GIBRALTAR (1977): L'histoire tectonique récente (Tortonien à Quaternaire) de l'Arc de Gibraltar et des bordures de la mer d'Alboran: conclusions générales, signification géodynamique des phénomènes observés, *Bull. Soc. Geol. Fr.*, **19** (13), **12**, 575-576 and 605-614.

HATZFELD, D. (1978): Etude sismotectonique de la zone de collision Ibéro-Maghrébine, *State Thesis*, University Joseph Fourier, Grenoble, pp. 281.

HATZFELD, D., V. CAILLOT, T.E. CHERKAOU, H. JEBLI and F. MEDINA (1993): Microearthquake seismicity and fault plane solutions around the Nekor strike-slip fault, Morocco, *Earth Planet. Sci. Lett.*, **120**, 31-41.

LEBLANC, D. and P. OLIVIER (1984): Role of strike-slip faults in the Betic-Rifian orogeny, *Tectonophysics*, **101**, 345-355.

LEE, W.H. and J.E. LAHR (1975): HYPO71 a computer program for determining hypocenter, magnitude and first motion pattern of local earthquakes, *U.S. Geol. Surv.*, Open-File Report 75-331.

LEVRET, A. (1995): Macrosismicité historique et contemporaine du Maroc en vue de l'évaluation de l'aléa sismique sur le site de Sidi Boulebra, in *Etude de Sites et de Faisabilité d'une Centrale Electronucleaire au Maroc*, Unpublished Report, Office Nationale de l'Electricité, Rabat, pp. 78.

MEDINA, F. (1995): Present-day state of stress in Northern Morocco from focal mechanism analysis, *J. Struct. Geol.*, **17**, 1035-1046.

MEDINA, F. and T.E. CHERKAOUI (1992): Mécanismes au foyer des séismes du Maroc et des régions voisines (1959-1986): conséquences tectoniques, *Eclogae Geol. Helv.*, **85**, 433-457.

MEGHRAOUI, M., J.-L. MOREL, J. ANDRIEUX and M. DAHMANI (1996): Tectonique Plio-Quaternaire de la chaîne tello-rifaine et de la mer d'Alboran. Une zone com-

plexe de convergence continent-continent, *Bull. Soc. Geol. Fr.*, **167** (1), 141-157.

MEZCUA, J. and J.M. MARTINEZ SOLARES (1983): Sismicidad del area Ibero-Mogrebi, *Instituto Geografico Nacional*, No. 203, pp. 301.

MINSTER, J.B. and T.H. JORDAN (1978): Present-day plate motions, *J. Geophys. Res.*, **83**, 5331-5354.

MORLEY, C.K. (1992): Notes on Neogene basin history of the Western Alboran Sea and its implications for the tectonic evolution of the Rif-Betic orogenic belt, *J. Struct. Geol.*, **14** (1), 57-65.

MOURIER, T. (1982): Etude géologique et structurale du massif des Bokkoya (Rif Oriental, Maroc), *Thèse de Troisième Cycle*, Univ. Paris XI, pp. 267.

NEIC (National Earthquake Information Centre) (1995): *Monthly Listing for May 1994*, U.S. Government Printing Office, Washington, pp. 28.

PLATT, J.P. and R.L.M. VISSERS (1989): Extensional collapse of thickened continental lithosphere: a working hypothesis for the Alboran Sea and Gibraltar arc, *Geology*, **17**, 540-543.

RAMDANI, M., B. TADILI and T. ELMRABET (1989): The present state of knowledge on historical seismicity of Morocco, in *Proceedings of the Symposium on Calibration of Historical Earthquakes in Europe and Recent Developments in Intensity Interpretation*, European Seismological Commission, Sofia, 23-28 August 1988, Instituto Geografico National, Madrid, 257-279.

REASENBERG, P. and D. OPPENHEIMER (1985): FPFIT, FPPLOT, and FPPAGE: FORTRAN computer programs for calculating and displaying earthquake fault-plane solutions, *U.S. Geol. Surv.*, Open-File Report, 85-739.

REBAI, S., H. PHILIP and A. TABOADA (1992): Modern tectonic stress field in the Mediterranean region: evidence for variation in stress directions at different scales, *Geophys. J. Int.*, **110**, 106-140.

ROUX, G. (1934): Notes sur les tremblements de terre ressentis au Maroc avant 1933, *Mém. Soc. Sci. Nat. Maroc*, **39**, 42-71.

SEBER, D. (1995): Lithospheric and upper mantle structure beneath Northern Morocco and Central Syria, *Ph.D. Thesis*, Cornell University, pp. 204.

TADILI, B. (1991): Etude du risque sismique au nord du Maroc, *State Thesis*, University Mohamed Premier, Fac. Sci. Oujda, pp. 231.

VEGAS, R. (1991): Present-day geodynamics of the Ibero-Maghrebian region, *Publ. Inst. Geogr. Nac.*, Madrid, Série Monografia, No. 8, 193-203.

VOGT, J. (1985): Révisions d'anciens séismes Ibéro-Magrébins, in *Etude de Sites et de Faisabilité d'une Centrale Eléctronucleaire au Maroc*, Unpublished Report, Office National de l'Electricité, Rabat, pp. 67.

WATTS, A.B., J.P. PLATT and P. BUHL (1992): Tectonic evolution of the Alboran Sea basin, *Basin Res.*, **5**, 153-177.

WEIJERMAARS, R. (1988). Neogene tectonics in the Western Mediterranean may have caused the Messinian Salinity Crisis and an associated glacial event, *Tectonophysics*, **148**, 211-219.

WORKING GROUP ON MACROSISMIC SCALES (1993): European Macroseismic Scale 1992 (up-dated MSK-scale), *Cahiers du Centre Européen de Géodynamique et de Séismologie*, pp. 79.

(received January 15, 1998;
accepted July 6, 1998)